A comparative investigation of different overlaps of the diode laser hardening in low-Carbon steel and stainless steel

Mojtaba Karamimoghadam [a], Mahmoud Moradi [a]*, Mohammad Azami [b]

[a] *School of Mechanical, Aerospace and Automotive Engineering, Faculty of Engineering, Environment and Computing, Coventry University, Gulson Road, Coventry, CV1 2JH, United Kingdom*

[b] *Mechanical Engineering Department, College of Engineering, University of Tehran, Tehran, Iran*

[*] *Corresponding author: ad6683@coventry.ac.uk*

Abstract

In this paper, the effect of laser overlap on the low-carbon and stainless steel are investigated. The analyzed samples are made of AISI 4130 low-Carbon steel and AISI 410 stainless steel with 50 % overlap. The used laser is an industrial high-power diode laser with a continuous wave and a maximum power of 2 kW. Samples are fabricated using optimized levels for laser power, focal plane position, and laser scanning speed, and the heat-treatment process is done after that. The parameters and conditions for the laser hardening process of both samples are the same situation. Then, the microstructure analysis is done using OM and SEM. Besides, the hardness of the samples is tested in the hardening depth and width. The study shows that the hardness is improved for both samples at the overlap area, up to 762 hv for AISI 4130 and 675 hv for AISI 410. Also, in both samples the amount of ferrite phase has decreased.

Keywords:

laser surface transformation hardening, Diode laser, heat-treatment, low-Carbon steel, stainless steel, Ferrite phase

Introduction

Nowadays, there is a growing demand for manufacturing accuracy and speed [1]. These needs recently obtained greater attention in automotive, aerospace, medical, and electronic industries, and deploying laser technology responded to these demands somewhat [2-6]. By

the advent of technology, lasers are widely used in additive manufacturing (AM), cutting, coating, clearing, drilling, hardening and etc. to act very effective in a fraction of a second [7-15]. Due to encompassing higher speed and accuracy levels than traditional hardening methods like induction hardening and furnace hardening, laser hardening owns priority in some cases [16-18]. In this method, the process parameters (like laser power, frequency, focal plane position (FPP), scanning speed, etc.) are determined, considering the laser type, then the heat-treatment process is conducted [19]. Low-Carbon steels are widely used in industries, so hardening of these parts seems necessary to prevent abrasion [20-24]. In this process, the laser beam should increase the surface temperature to the phase transformation point without surface melting and crack formation. However, in some cases, these defects are inevitable, and we should find a way to prevent that by implementing suitable parameters and material behavior scrutiny [25-30].

The laser surface transformation (LSTH) leads to a fine-grained structure after laser hardening, as the self-quenching occurs in the hardened part, which has no undesirable result on the part's properties [31]. Due to encompassing characteristics like wall-plug efficiency, a rectangular laser beam from top-hat intensity, and better heat absorption, using high power diode lasers are preferred to use CO2 and Nd:YAG laser for LSTH [32, 33]. The LSTH of stainless steel is an excellent technique in the industrial components to make the surface properties better in order to improve their wear and corrosion resistance [34-36]. Escudero and Bello [37] used microstructure analysis and Vickers hardness to evaluate AISI 420 steel LSTH. Mahmoudi et al. [38] examined the variation of hardness and hardened area dimension by changing input parameters in the LSH process of AISI 420 by an industrial Nd:YAG laser. They also compared the properties of samples hardened using this method with hardened samples using traditional techniques. Zirehpour et al. [39] also improved the wear and hardness behavior of AISI 420 steel specimens using an industrial Nd:YAG laser. Netprasert et al. [40] investigated the LSH of AISI 420 steel using a Nanosecond pulse laser. Babu et al. [41] examined the influence of LSH process parameters in EN25 steel samples. Adel [42] also conducted the LSH process on Ck45 steel samples. In this research, the effect of Laser power (LP) and laser scanning speed (LS) was analyzed on the wear behavior. Sun et al. [43] also numerically simulated the LSH of 42CrMo cast steel, considering industrial Nd:YAG Laser considered the laser source and verified the results with experimental data. An investigation on LSH of AISI 1045 steel also was done by Li et al. [44]. In this study, the effect of beams' distribution quality on the steel surface was examined. In other researches,

LSH on commercial steels like 4Kh5MFS, AISI H13, VK6, and C80U were studied [45-48]. For 4140 steel, a comparison between experimental and numerical results of the LSH process was made by Cordovilla et al. [49]. The application of HPDL as a high precision tool in the LSH process was also investigated in some studies [50, 51]. Chang et al. [52] investigated the LSH process of 50CrMo4 steel by implementing continuous-wave laser and pulsed lasers. This research aimed to reach maximum hardness with the lowest power. Besides, a comparison was made on the micro-hardness, geometrical dimensions, and surface quality of the LSH process of different lasers. LSH process does not necessarily make the mechanical and material properties better. For instance, the LSH samples showed poor corrosion behavior in research conducted by Maharjan et al. [53].

In this paper, by using the LSH technique by a diode laser, the overlapping of AISI 4130 steel and AISI 410 steel were investigated. The detailed analysis of the hardened area seems vital, as it potentially contains different hardening defects. In this research, Low Carbon steel was hardened using a high-power industrial 2 kW Diode laser, and the effect of 50% overlap on the samples were examined. Additionally, for the AISI 4130 sample, laser surface hardening by three tracks, has been interacted to show better the wide laser hardening process. Then, the microstructure analysis is done using OM and SEM. Besides, the hardness of the samples is tested in the hardening depth and width. The study shows that the hardness is improved for both samples at the overlap area, up to Hv762.

2. EXPERIMENTAL MATERIALS AND METHODS

The chemical composition of AISI 4130 and AISI 410 was measured by X-ray fluorescence (XRF) in three separate parts of the base metal. In Table 1 Wt. % of each elements is shown. The etching solution has been used to show the microstructure of AISI 4130 and AISI 410 after LSTH. The solution is made of 5 gr of Picric acid and about 95 cc of Ethanol for AISI 4130 and the solution for AISI 410 is villa's reagent (C2H5OH 100cc, Hcl 5cc, C6H3N3O7 2gr) [54]. After etching samples should wash with water and Ethanol very well to clear any dust and dirt from the top of the samples' surfaces. Samples for LSTH were cut in 6.5 cm in the roll shape and the top sections were faced by lathe machine. The LSTH process is depicted on Figure 1. The laser in this study is 2KW diode laser with continuous wave length.

Table 1. Chemical composition of AISI 4130 and AISI 410 (Wt. %)

STEEL	C	Si	Ni	Mn	P	S	Cu	Cr	Mo	Al	V	Fe
AISI 4130	0.25	0.3	0.05	0.87	0.016	0.03	0.06	1.01	0.25	0.024	0.012	BA
AISI 410	0.15	0.28	0.12	0.51	0.018	0.024	0.11	13.5	0.03	0.008	0.021	BA

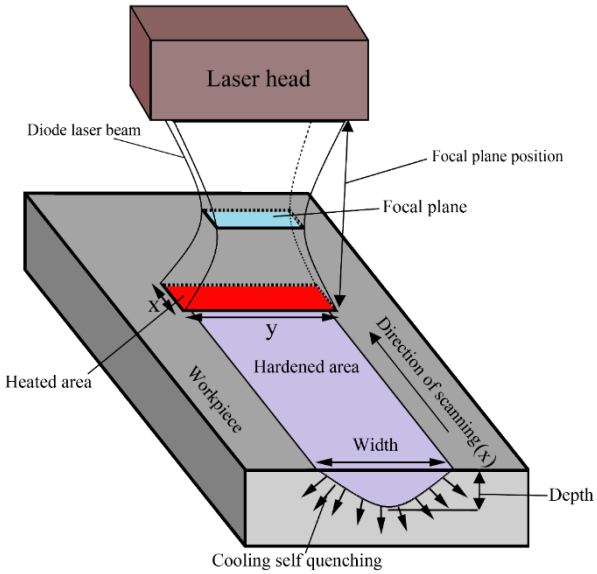

Figure 1 The LSTH schematic by diode laser [55]

After well invetigation on the laser input parameters in LSTH, some input parameters were selected such as Laser power 1490 W, FPP 62 mm, and scanning speed 4.45 mm/s. By mentioned parameters overlap of the LSTH process were applied in 50 % and Figure 2 shows the 50% overlap for LSTH of AISI 4130.

By dividing the beam length (x) to laser scanning speed, the interaction time has been generated in Equation 1. Also, in Figure 1 the beam length is illustrated. The beam density is another important parameter on the LSTH and it can be calculated by Equation 2 [55]:

Interaction time= Beam length (x)/Laser speed (1)

Beam density= Power/ Beam area (2)

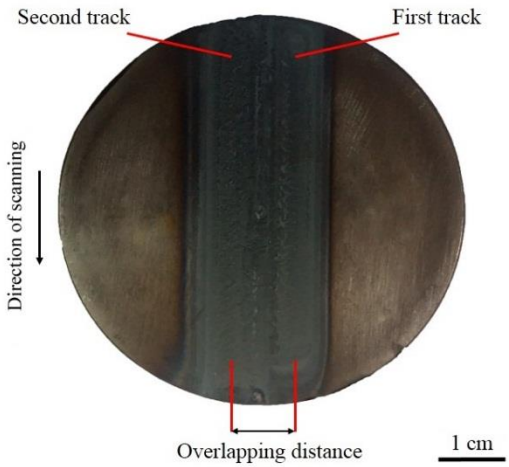

Figure. 2. Image of the overlap laser hardened samples (overlap 50%)

3 RESULTS AND DISCUSSION

Table 2 depicts some results of the LSTH process. In the steels, the ferrite percentage has a critical role because this phase of steel defines the hardness and other mechanical properties. On the other hand, by LSTH all parts of the surface may have a proper interaction by the laser beam. Meanwhile huge part of the surface has a treatment by the laser, it might remain some ferrite phase after air quenching. In Table 2 shows Ferrite Percentage which is less than Ferrite Percentage before overlapping for both materials. This phenomenon occurs because of some reasons, for example, in the width of LSTH the far parts of the laser beam, especially in the edges, the heat input is lower than the center of laser beam concentration, so the edges may not well be treated by laser beam and after quenching process by air some ferrite phase remains. Meanwhile, by overlapping processes, these parts may heat treat again and ferrite phases change to martensitic phases. In the AISI 4130, the ferrite phase is 0.27% which is less than 9.92% before overlapping. This phenomenon was created higher micro-hardness and the results are shown in Table 2. The highest micro-hardness for AISI 4130 was measured about 762 Hv for 50% overlap. Also, In Figure 3, the macro scale of the 50% overlap for AISI 4130 and AISI 410 are shown. The ferrite percentage has been measured by Clemex software and the geometry of hardened area has been calculated by ImageJ software.

Table 2. The overlap characterization

Samples	Input			Output				
	Power (w)	Scanning speed (mm/s)	FPP (mm)	Overlapped width (µm)	Ferrite Percentage before overlapping (%)	Ferrite Percentage (%)	Max. Hardness in the overlap area before overlapping (HV0.1)	Overlap Max. hardness (HV0.1)
AISI 4130	1490	4.45	62	1170	9.92	0.27	483	762
AISI 410				970	8.7	0.95	410	675

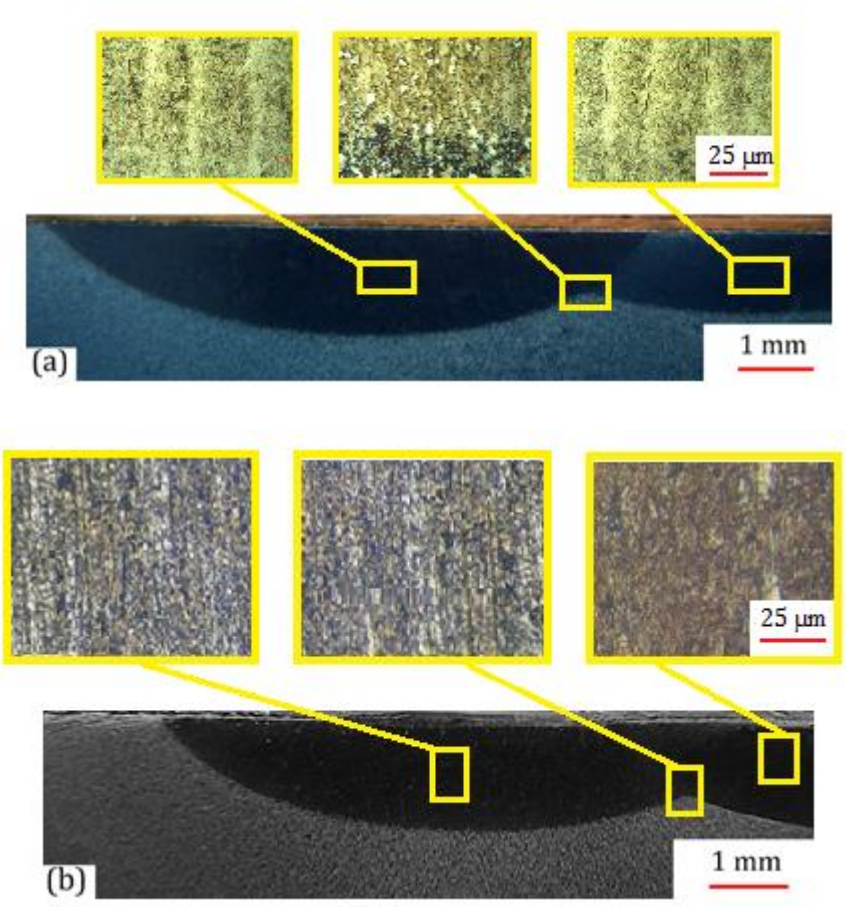

Figure 3. Macro and micro scale of overlap samples a) The 50% overlap of AISI 4130 b) The 50% overlap of AISI 410

Figure 4 the micro-hardness diagrams for 50% overlap are depicted. In Figure 4, it is completely clear that for both metals the micro-hardness have increased and also, exactly in the center of the first track of LSTH, the ferrite percentage is less than the second track of

laser hardening. It can be seen that in Table 2, the ferrite percentage is lower than before the second track. This is because re-treatment has removed ferrite and created martensitic phase after air quenching.

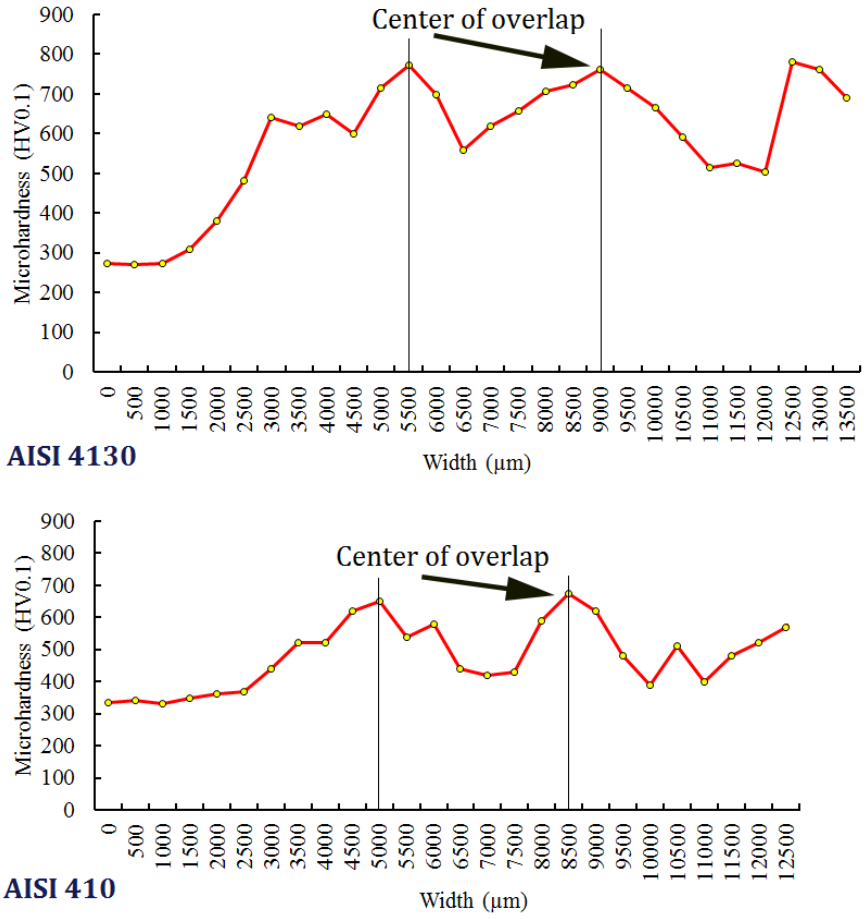

Figure. 4. Micro-hardness for AISI 4130 and AISI 410

In Figure 5, SEM analysis of overlap samples is shown. Base on the brighter parts which are depicted the ferrite phase into martensitic structures, the martensitic phase more than the ferrite phase. In Figure 6a and b, the ferrite phase has been geared into the tough structure of the martensitic phase of AISI 4130 which leads to a decrease in micro-hardness. By comparison Figure 5-c and d, it is obvious that the ferrite phase in AISI 410 has decreased and is not very much. Finally, after analyzing the overlap of samples, the three track LSTH of one of the samples was hardened and it is shown at Figure 6.

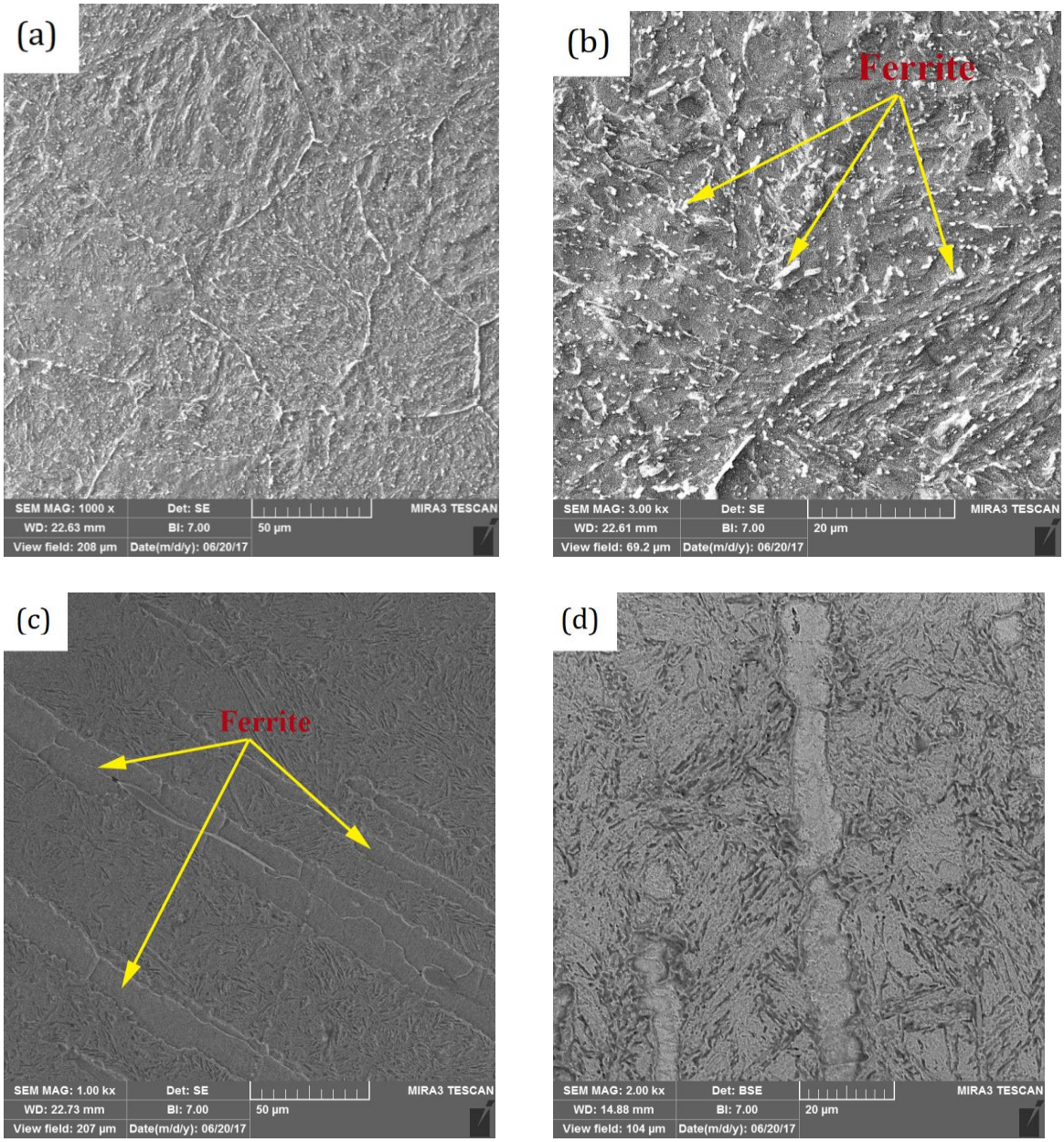

Figure 5 a & b) SEM for 50% overlap sample of AISI 4130 c & d) SEM for 50% overlap sample of AISI 410

(a) (b)

Figure 6. Three track LSTH of AISI 4130 a) schematic and the laser scanning direction b) the sample after wide surface hardening process

4. CONCLUSIONS

In this paper, the effect of laser overlap on low-carbon steel and stainless steel are investigated. The analyzed samples are made of AISI 4130 low-Carbon steel and AISI 410 with 50 % overlap. Results were shown that the micro-hardness in the 50% overlap sample of AISI is 762 hv and in AISI 410 overlap is 675 hv. The concentration of this study is to show the role of ferrite transformation after the overlapping processes. Also, the rate of ferrite percentage in the edge of laser hardened traces decreased significantly. The percentage of ferrite in AISI 4130 and AISI 410 before the overlap process were 9.92 and 8.7 percent respectively and after overlap declined to 0.27 and 0.95 percent. The overlap has a positive effect on decreasing the ferrite phase after the second track of the LSTH.

References:

[1] E. Kannatey, and Jr. Asibu. *Principles of Laser Materials Processing*. New Jersey: Published by John Wiley and Sons, Hoboken. 2009.

[2] Savin, I.A., 2021. Laser Hardening of Stamps in the Conditions of a Large Engineering Company. In Defect and Diffusion Forum (Vol. 410, pp. 450-455). Trans Tech Publications Ltd.

[3] Pramanik, D., Kuar, A.S., Sarkar, S. and Mitra, S. Enhancement of sawing strategy of multiple surface quality characteristics in low power fiber laser micro cutting process on titanium alloy sheet. *Optics & Laser Technology* **122** (2020), 105847.

[4] Amne Elahi, M., Koch, M., Bardon, J., Addiego, F. and Plapper, P., 2021. Failure mechanism analysis based on laser-based surface treatments for aluminum-polyamide laser joining. Journal of Materials Processing Technology, 298.

[5] Liu, F., Xu, B., Song, K., Tan, C., Zhao, H., Wang, G., Chen, B. and Song, X., 2021. Improvement of penetration ability of heat source for 316 stainless steel welds produced by alternating magnetic field assisted laser-MIG hybrid welding. Journal of Materials Processing Technology, p.117329.

[6] Metelkova, J., Vanmunster, L., Haitjema, H., Ordnung, D., Kruth, J.P. and Van Hooreweder, B., 2021. Hybrid dual laser processing for improved quality of inclined up-facing surfaces in laser powder bed fusion of metals. Journal of Materials Processing Technology, 298, p.117263.

[7] Speidel, A., Wadge, M.D., Gargalis, L., Cooper, T.P., Reynolds, W., Grant, D., Hague, R., Clare, A.T. and Murray, J.W., 2021. The interaction of volatile metal coatings during the laser powder bed fusion of copper. Journal of Materials Processing Technology, p.117332.

[8] Travessa, D.N., Guedes, G.V.B., de Oliveira, A.C., Cardoso, K.R., Roche, V. and Jorge Jr, A.M., 2021. The effect of surface laser texturing on the corrosion performance of the biocompatible β-Ti12Mo6Zr2Fe alloy. Surface and Coatings Technology, 405, p.126628.

[9] Moradi, M., Moghadam, M.K. and BEIRANVAND, Z., 2021. CO 2 Laser Engraving of Injection Moulded Polycarbonate: Experimental Investigation. Lasers in Engineering (Old City Publishing), 48.

[10] Mucciaroni, L.R. and Vivas, M.G., 2021. Efficient Yet Accessible Arduino-based Control System for Laser Microfabrication of Photonic Platforms. Lasers in Manufacturing and Materials Processing, pp.1-14.

[11] Zhang, H., Xu, M., Kumar, P., Li, C., Liu, Z. and Zhang, Y., 2021. Fatigue life prediction model and entropy generation of 304L stainless steel fabricated by selective laser melting. Journal of Materials Processing Technology, 297, p.117279.

[12] Fironov, Y.S., Melnikov, I.V., Nadezhdin, E.R. and Tokarev, V.N., 2021, March. Laser drilling a highly porous aluminosilicate ceramics. In High-Power Laser Materials Processing: Applications, Diagnostics, and Systems X (Vol. 11679, p. 116790F). International Society for Optics and Photonics.

[13] Zhang, X., Li, D. and Geng, J., 2021. An approach to reduce stress and defects: a hybrid process of laser cladding deposition and shot peening. Rapid Prototyping Journal.

[14] Mishra, Y.K., Mishra, S. and Jayswal, S.C., 2021. Parametric Analysis and Optimization of Inclined Laser Percussion Drilling of Carbon Fiber Reinforced Plastic Using Solid-State Nd: YAG Laser. Lasers in Manufacturing and Materials Processing, pp.1-30.

[15] DZOGBEWU, T.C., 2021. Laser powder bed fusion of Ti6Al4V-xCu: Process parameters. Journal of Metals, Materials and Minerals, 31(2), pp.62-70.

[16] Maharjan, N., Zhou, W. and Wu, N., 2020. Direct laser hardening of AISI 1020 steel under controlled gas atmosphere. Surface and Coatings Technology, 385, p.125399.

[17] Chichenev, N.A., Gorbatyuk, S.M., Naumova, M.G. and Morozova, I.G., 2020. Using the similarity theory for description of laser hardening processes. CIS Iron and Steel Review, 19, pp.44-47.

[18] Fakir, R., Barka, N. and Brousseau, J., 2018. Case study of laser hardening process applied to 4340 steel cylindrical specimens using simulation and experimental validation. Case Studies in Thermal Engineering, 11, pp.15-25.

[19] Ponticelli, G.S., Guarino, S. and Giannini, O., 2020. An optimal genetic algorithm for fatigue life control of medium carbon steel in laser hardening process. Applied Sciences, 10(4), p.1401.

[20] Barka, N., Sattarpanah Karganroudi, S., Fakir, R., Thibeault, P. and Feujofack Kemda, V.B., 2020. Effects of laser hardening process parameters on hardness profile of 4340 steel spline—an experimental approach. Coatings, 10(4), p.342.

[21] Su, W., Zhou, T., Zhang, P., Zhou, H. and Li, H., 2018. Effect of distribution of striated laser hardening tracks on dry sliding wear resistance of biomimetic surface. Optics & Laser Technology, 98, pp.281-290.

[22] Morozov, E., Ablyaz, T., Muratov, K., Shlykov, E. and Smolentsev, E., 2020. Laser hardening of copper-iron pseudoalloy. Engineering Solid Mechanics, 8(2), pp.83-92.

[23] Wagh, S.V., Bhatt, D.V., Menghani, J.V. and Bhavikatti, S.S., 2018. Effects of laser hardening process parameters on the mechanical and wear properties of ck45 steel using an orthogonal array. International journal of modern manufacturing technologies, 10, pp.86-93.

[24] Sundqvist, J., Manninen, T., Heikkinen, H.P., Anttila, S. and Kaplan, A.F.H., 2018. Laser surface hardening of 11% Cr ferritic stainless steel and its sensitisation behaviour. Surface and Coatings Technology, 344, pp.673-679.

[25] Maharjan, N., Zhou, W., Zhou, Y., Guan, Y. and Wu, N., 2019. Comparative study of laser surface hardening of 50CrMo4 steel using continuous-wave laser and pulsed lasers with ms, ns, ps and fs pulse duration. Surface and Coatings Technology, 366, pp.311-320.

[26] Al-Sayed, S.R., Elshazli, A.M. and Hussein, A.H.A., 2020. Laser surface hardening of Ni-hard white cast iron. Metals, 10(6), p.795.

[27] Li, C., Yin, C. and Xu, X., 2021. Hybrid optimization assisted deep convolutional neural network for hardening prediction in steel. Journal of King Saud University-Science, 33(6), p.101453.

[28] Jiao, Y., Brousseau, E., Kosai, K., Lunt, A.J., Yan, J., Han, Q., Zhu, H., Bigot, S. and He, W., 2021. Softening and hardening on a Zr-based bulk metallic glass induced by nanosecond laser surface melting. Materials Science and Engineering: A, 803, p.140497.

[29] Zhang, J., Huang, T., Shen, Z., Su, H., Zhang, J. and Liu, L., 2021. Enhanced structural refinement on eutectic medium-entropy alloy CrCoNiNb0. 48 by laser remelting. Materials Letters, p.130710.

[30] Guo, D., Yu, D., Zhang, P., Song, W., Zhang, B. and Peng, K., 2021. Laminar plasma jet surface hardening of P20 mold steel: Analysis on the wear and corrosion behaviors. Surface and Coatings Technology, 415, p.127129.

[31] A. Sim, Ch. Park, N. Kang, Y. Kim, E. Chun. Effect of laser-assisted nitriding with a high-power diode laser on surface hardening of aluminum-containing martensitic steel. *Optics & Laser Technology* **116** (2019), 305-314.

[32] N. Maharjan, W. Zhou, Y. Zhou, Y. Guan, N. Wu. Comparative study of laser surface hardening of 50CrMo4 steel using continuous-wave laser and pulsed lasers with ms, ns, ps and fs pulse duration. *Surface and Coatings Technology* **366** (25) (2019), 311-320.

[33] Zhu, H., Fu, X., Fan, S., Liang, L., Lin, X. and Ning, Y. The conversion from a Gaussian-like beam to a flat-top beam in the laser hardening processing using a fiber coupled diode laser source. *Optics & Laser Technology* **125** (2020), 106028.

[34] L. Pan, C. T. Kwok, K. H. Lo. Enhancement in hardness and corrosion resistance of AISI 420 martensitic stainless steel via friction stir processing. *Surface and Coatings Technology* **15** (357) (2019), 339-347.

[35] Moradi, M., Arabi, H., Moghadam, M.K. and Benyounis, K.Y. Enhancement of surface hardness and metallurgical properties of AISI 410 by laser hardening process; diode and Nd: YAG lasers. *Optik* **188** (2019), 277-286.

[36] S. D. Nath, H. Irrinki, G. Gupta, M. Kearns, S. Atre. Microstructure-property relationships of 420 stainless steel fabricated by laser-powder bed fusion. *Powder Technology* **343** (1) (2019), 738-746.

[37] M. L. EscuderoJ, M. Belló. Laser surface treatment and corrosion behaviour of martensitic stainless AISI 420 steel. *Materials Science and Engineering: A* **2** (1) (1992), 227-233.

[38] B. Mahmoudi, M. J. Torkamany, A. R. S. Rouh Aghdam, J. Sabbaghzade. Laser surface hardening of AISI 420 stainless steel treated by pulsed Nd:YAG laser. *Materials & Design* **31** (5) (2010), 2553-2560.

[39] Gh. Zirepour, R. Shojaa Razavi. Evaluation of Electrochemical Corrosion Effects of AISI 420 Steel after Laser Surface hardening. *Journal of Science and surface engineering* **22** (2014) 71-79.

[40] O. Netprasert V. Tangwarodomnukun, Ch. Dumkum. Surface Hardening of AISI 420 Stainless Steel by Using a Nanosecond Pulse Laser. *Materials Science Forum* **911** (2018), 44-48.

[41] D. Babu, G. Buvanashekaran. Experimental studies on the microstructure and hardness of laser transformation hardening of low alloy steel. *Transactions of the Canadian Society for Mechanical Engineering* **36** (2012), 241-258.

[42] Adel K. M. Enhancement of Dry Sliding Wear Characteristics of CK45 Steel Alloy by Laser Surface Hardening Processing. *Procedia Materials Science* **6** (2014), 1639-1643.

[43] P. Sun, Sh. Li, G. Yu, X. He, C. Zheng, W. Ning. Laser surface hardening of 42CrMo cast steel for obtaining a wide and uniform hardened layer by shaped beams. *Int J Adv Manuf Technol* **70** (2014), 787-796.

[44] R .Li, Y. Jin, Z. Li, K. Qi. A Comparative Study of High-Power Diode Laser and CO_2 Laser Surface Hardening of AISI 1045 Steel. *Journal of Materials Engineering and Performance*, **23** (2014), 3085-3091.

[45] I. A. Pinahin, V. A. Chernigovskij, A. A. Bracihin, and M. A. Yagmurov. Improvement of Wear Resistance of VK6, VK8, T5K10 and T15K6 Hard Alloys by Volume Pulsed Laser Hardening. *Friction and wear* **36** (2015), 330-333.

[46] A. V. Aborkin, V. E. Vaganov, A. N. Shlegel, I. M. Bukarev. Effect of laser hardening on die steel microhardness and surface quality. *Metallurgist* **59** (2015), 619-625.

[47] A. Bie´n, M. Szkodo. Surface treatment of C80U steel by long CO_2 laser pulses. *Journal of Materials Processing Technology* **217** (2015), 114-121.

[48] G. Telasang, J. DuttaMajumdar, G. Padmanabham, I.Manna. Wear and corrosion behavior of laser surface engineered AISI H13 hot working tool steel. *Surface & coatings technology* **261** (2015), 69-78.

[49] F. Cordovilla, A. G. Beltra, P. Sancho, J. Dom´ınguez, L. R. de Lara, J. Oca˜na. Numerical/experimental analysis of the laser surface hardening with overlapped tracks to design the configuration of the process for Cr-Mo steels. *Materials & Design* **102** (2016), 225-237.

[50] S. Guarino, M. Barletta, A. Afilal. High Power Diode Laser (HPDL) surface hardening of low carbonsteel: Fatigue life improvement analysis. *Journal of Manufacturing Processes* **28** (2017), 266-271.

[51] Moradi, M., Moghadam, M. K., Fallah, M. M., Hesadi, M. Investigating the Effect of High Power Diode Laser (HPDL) Surface Treatment on the Corrosion Behavior of 17-4 PH Martensitic Stainless Steel. Lasers in Engineering (Old City Publishing), **46** (2020), 245-156.

[52] N. Maharjan, W. Zhou, Y. Zhou, Y. Guan, N. Wu. Comparative study of laser surface hardening of 50CrMo4 steel using continuous-wave laser and pulsed lasers with ms, ns, ps and fs pulse duration. *Surface and Coatings Technology* **366** (2019), 311-320.

[53] N. Maharjan, V. K. Murugan, W. Zhou, M. Seita, Corrosion behavior of laser hardened 50CrMo4 (AISI 4150) steel: A depth-wise analysis. *Applied Surface Science* **494** (2019), 941-951.

[54] Vander Voort, G.F., Lampman, S.R., Sanders, B.R., Anton, G.J., Polakowski, C., Kinson, J., Muldoon, K., Henry, S.D. and Scott Jr, W.W., 2004. ASM handbook. Metallography and microstructures, 9, pp.44073-0002.

[55] Moradi, M. and KaramiMoghadam, M., 2019. High power diode laser surface hardening of AISI 4130; statistical modelling and optimization. Optics & Laser Technology, 111, pp.554-570.

Highlights:

- Laser surface transformation hardening
- Overlap of hardening after laser process of AISI 4130 and AISI 410
- Wide laser surface transformation hardening by Diode Laser
- Laser power, focal plane position and speed considered for the laser